ACSNANO
www.acsnano.org
ARTICLE

P-Doped Porous Carbon as Metal Free Catalysts for Selective Aerobic Oxidation with an Unexpected Mechanism

Mehulkumar A. Patel,[†] Feixiang Luo,[‡] M. Reza Khoshi,[†] Emann Rabie,[†] Qing Zhang,[§] Carol R. Flach,[†] Richard Mendelsohn,[†] Eric Garfunkel,[‡] Michal Szostak,*[,†] and Huixin He*[,†]

[†]Department of Chemistry, Rutgers University, 73 Warren Street, Newark, New Jersey 07102, United States
[‡]Department of Chemistry and Chemical Biology, Rutgers University, 610 Taylor Road, Piscataway, New Jersey 08854, United States
[§]Department of Chemistry, Jilin University, 2699 Qianjin Street, Changchun 130012, P. R. China

Supporting Information

ABSTRACT: **An extremely simple and rapid (seconds) approach is reported to directly synthesize gram quantities of P-doped graphitic porous carbon materials with controlled P bond configuration. For the first time, it is demonstrated that the P-doped carbon materials can be used as a selective metal free catalyst for aerobic oxidation reactions. The work function of P-doped carbon materials, its connectivity to the P bond configuration, and the correlation with its catalytic efficiency are studied and established. In direct contrast to N-doped graphene, the P-doped carbon materials with higher work function show high activity in catalytic aerobic oxidation. The selectivity trend for the electron donating and withdrawing properties of the functional groups attached to the aromatic ring of benzyl alcohols is also different from other metal free carbon based catalysts. A unique catalytic mechanism is demonstrated, which differs from both GO and N-doped graphene obtained by high temperature nitrification. The unique and unexpected catalytic pathway endows the P-doped materials with not only good catalytic efficiency but also recyclability. This, combined with a rapid, energy saving approach that permits fabrication on a large scale, suggests that the P-doped porous materials are promising materials for "green catalysis" due to their higher theoretical surface area, sustainability, environmental friendliness, and low cost.**

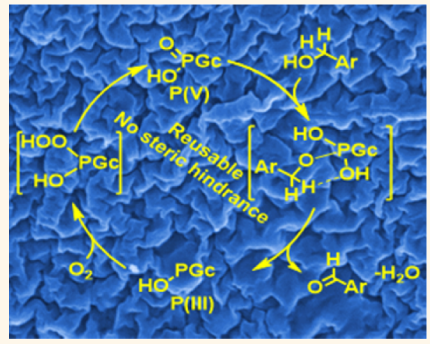

KEYWORDS: *phosphorus doped carbon, aerobic oxidation, alcohol oxidation reaction, carbon catalyst, microwave assisted fabrication*

Catalytic oxidation of inexpensive and widely available chemicals to produce high value-added chemicals remains a significant task in many important current industrial and fine-chemical processes. Ideal catalytic oxidation processes would use nontoxic sustainable catalysts and the most environmentally benign and abundant oxidants, such as molecular oxygen (O_2), with good conversion and selectivity. A wide range of homogeneous and heterogeneous transition metal-based catalysts have been developed for these reactions. Unfortunately, many metals are not widely available and/or are toxic, which presents sustainability and environmental challenges. For these reasons, there is ever increasing interest in developing sustainable and eco-friendly, metal-free "carbon based catalysts", including graphene and other nanocarbon based catalysts.[1−5]

Compared to traditional metal based catalysts, carbon based materials provide additional advantages because the existence of giant π structures promotes strong interactions with various reactants. More importantly, its physicochemical and electronic properties, which in principle determine the catalytic properties of a material, can be tailored and fine-tuned by molecular engineering and/or heteroatomic doping.[6] A plethora of reports have demonstrated that doping of heteroatoms into graphene and other carbon based materials gives rise to enhanced performance in electrocatalytic oxygen reduction reaction (ORR), when compared to their undoped analogues.[7−10] Compared to ORR, studies that use doped and/or co-doped carbon materials as catalysts for selective organic synthesis are in their early stages of development, although a great potential has already been demonstrated.[11] Importantly, these carbocatalysts merge the benefits of green synthesis with heterogeneous reaction conditions, which greatly simplifies workup conditions and is particularly attractive from an industrial standpoint. However, there are few reports demonstrating that carbon based materials match the efficiency

Received: November 8, 2015
Accepted: January 11, 2016
Published: January 11, 2016

DOI: 10.1021/acsnano.5b07054
ACS Nano 2016, 10, 2305−2315

and recyclability of transition metal catalysts.[11] On the other hand, limited "types" of graphene and carbon materials have been explored so far.[2,12−15] The majority of the research has been focused on graphene oxide (GO) possibly due to its large availability.[16−18] Carbon materials doped with nitrogen (N) and N co-doped with other heteroatoms have been explored for C−H activation and aerobic alcohol oxidation.[12,15,19,20] Among three types of nitrogen species doped into the graphene lattice, pyridinic N, pyrrolic N, and graphitic N, the graphitic sp^2 N species were established to be catalytically active centers for the observed catalytic performance. However, the requirement of high temperature to fabricate the graphitic sp^2 N violates the original idea for energy saving and sustainability.[21] Furthermore, the planar structure of graphitic sp^2 N brings difficulties in overcoming substrate steric hindrance effects, which causes limited catalytic reaction scope of N-doped carbon materials.[20,22]

Recently, growing interest has emerged in phosphorus (P) doped carbon materials.[23−26] P has the same number of valence electrons as N, making P-doped carbon materials also electron rich.[24] The polarity of the C−P bond is opposite to that of the C−N bond due to lower electronegativity of P atoms (2.19) than C (2.55), making P partially positively charged and possibly the catalytic sites,[27,28] instead of the neighboring C atoms as in the N-doped carbon materials.[12,15,19] Furthermore, as the diameter of P is much larger than C, P-doping results in more local structural distortion of the hexagonal carbon framework and in such a configuration, P protrudes out of the graphene plane.[27,28] Finally, when compared with N-doping, distinct effects by P-doping may also arise from the additional vacant 3d orbitals and the valence electrons in the third shell. All these characteristics empower P-doped carbon materials to overcome the steric hindrance effects encountered in N-doped carbon materials.[12,20] However, experimentally, most of the approaches for P-doping necessitate accompanying O doping, forming various P and O containing functional groups.[25,26,29] How these functional groups, and the bonding configuration of P in a carbon matrix, influence the electronic property and therefore its catalytic performance remains unknown. Furthermore, most of the P-doped materials were fabricated *via* high temperature annealing for long period of time in an inert environment, which also violates the original idea for energy saving and sustainability.

Herein, we report an extremely simple and rapid (seconds) approach to directly synthesize gram quantities of P-doped porous carbon materials from abundant biomass molecules. The work function of P-doped carbon materials and its connectivity to the P bond configuration in the carbon matrix have been studied *via* PeakForce Kelvin probe force microscopy (PF KPFM). Most significantly, the capability of the P-doped carbon materials as metal free catalysts for aerobic oxidation reactions have been demonstrated for the first time. As expected, unlike N-doped carbon material, the steric problem does not exist for P-doped carbon materials. The P-doped materials can efficiently catalyze aerobic oxidation of both primary and secondary benzyl alcohols to the corresponding aldehydes or ketones. A kinetic study shows that the P-doped carbon material has activation energy of ~49.6 kJ mol^{-1} for benzyl alcohol oxidation, which is lower than N-doped carbon (~56.1 kJ mol^{-1})[20] catalyst and similar to Ru based catalysts (~48 kJ mol^{-1}).[30,31] Further, to our surprise, the P-doped carbon materials with higher work functions show higher capability in catalyzing aerobic oxidation reactions, which is opposite to the trend when N-doped carbon materials are used as metal free catalysts for aerobic oxidation reactions[20,32] and electrochemical catalysts for ORR.[33] The P-doped materials also exhibit a different selectivity rule for electron rich and electron deficient molecules compared to other heteroatom doped carbon materials.[20,34] The reaction pathway was studied to understand these questions. We found that molecular oxygen is not involved in the first step of aerobic oxidation of benzyl alcohol; however, it is required to regenerate the catalytic sites on the P-doped carbon materials. The unique and unexpected catalytic pathway endows the P-doped carbon materials with not only good catalytic efficiency but also recyclability, which is a major challenge in GO based catalysis.[18,35] This, combined with rapid and energy saving approach to be able to fabricate the material in a large scale, suggests that the P-doped porous carbon is promising material for "green catalysis" due to their higher theoretical surface area, sustainability, environmental friendliness, and low cost.

RESULTS AND DISCUSSION

In this approach, a novel sustainable biomass molecule, phytic acid, a well-known antinutrient molecule in food, was chosen as our starting material. Phytic acid is a snowflake-like molecule, containing 6 phosphorous acid "arms" (Scheme 1). The

Scheme 1. Schematic Drawing of PGc Synthesis from Phytic Acid by Microwave Heating

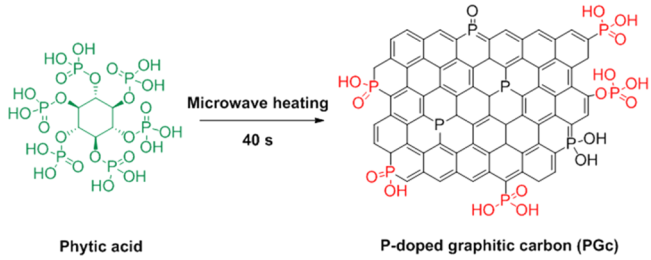

existence of both high levels of C and P in one molecule ensures uniform P doping in the fabricated carbon materials. Most importantly, phytic acid strongly absorbs microwave energy. Therefore, the as-purchased phytic acid solution can be directly used for the fabrication of P-doped graphitic carbon product (PGc) with microwave energy without requirement of preheating and drying treatment and without adding additional microwave absorber.[36,37] This is very different from most biomass molecules and organic materials that are typically transparent to microwave energy, thus prohibiting their direct use for microwave carbonization. Using microwave heating instead of traditional heating ensures that the approach is sustainable and has low energy cost. Furthermore, the fabrication can be performed in air, under ambient conditions without the requirement of inert environment, which makes this approach even more cost-effective and convenient.

Figure 1 shows a scanning electron microscope (SEM) image of the as-fabricated PGc which is obtained by subjecting the as-purchased phytic acid solution (50 wt % in water) to short (40 s) microwave irradiation. PGc has a very unique structure in which a porous carbon monolith sandwiched by two highly wrinkled graphene-like sheets (Figure 1). The wrinkled structure is possibly the result of P doping and the larger diameter of P atoms compared to C atoms which induce local geometrical distortion in the carbon network. Indeed, X-ray

DOI: 10.1021/acsnano.5b07054
ACS Nano 2016, 10, 2305−2315

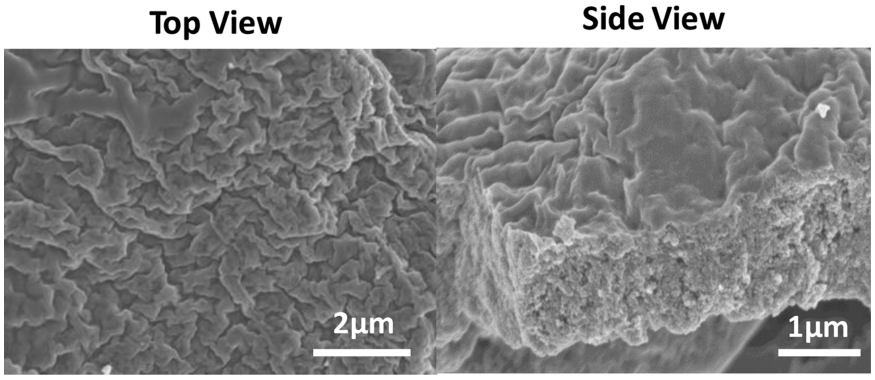

Figure 1. Scanning electron microscope (SEM) images of the as-fabricated PGc catalyst.

photoelectron spectroscopy (XPS) measurement (Figure S1 and Table S1) shows that PGc incorporates 4.9 atomic % P, demonstrating that P is doped in the carbon matrix. Raman spectroscopy was also used to characterize the PGc material. As shown in Figure S3, the Raman spectra of the PGc shows G band (~1594 cm^{-1}) and D band (~1312 cm^{-1}). The presence of G band (1594 cm^{-1}) confirms the presence of graphitic sp^2 carbon in its structure. The intensity of D band (1312 cm^{-1}) and the intensity ratio (I_D/I_G) of D and G band are very similar to those of GO and reduced GO (rGO). These results are consistent with the previous reports that incorporation of heterogeneous dopants, such as P and N, breaks the hexagonal symmetry of the graphene plane, which leads to the high intensity of D band in their Raman spectra.[9,10,34] Furthermore, the material has a large surface area (~1200 m^2/g), measured *via* Brunauer–Emmett–Teller (BET) (Figure S4) and it is highly thermally stable demonstrated from thermo gravimetric analysis (Figure S5). All these features combined with the ease of large-scale production should lead to a wide range of applications of this material, including as metal free catalysts.

We first studied the catalytic efficiency of PGc for selective oxidation of benzyl alcohol to benzaldehyde in aqueous solution at different temperatures (Table 1). The conversion increased with the reaction temperatures and it reached 48% at 100 °C without losing the selectivity to aldehyde (>99%, *cf.* benzoic acid) (entries 1–4). In a control experiment without PGc (entry 6) or with reduced GO (rGO) as the catalyst (entry 7), negligible conversion of benzyl alcohol is achieved, demonstrating the critical role of PGc in this reaction. It is worthy to mention that the conversion is 33.4% at 60 °C with >99% selectivity to benzaldehyde (entry 11), which is approximately three times higher than the conversion (entry 12) when N-doped graphene was used as the catalyst under almost identical reaction conditions (catalyst loading 300 wt %, and reaction time 10 h, except the reaction was performed at slightly higher temperature 70 °C for N-doped graphene).[20] Detailed kinetic study of the selective oxidation of benzyl alcohol to benzaldehyde in aqueous solution by PGc catalyst was also performed. Figure S6 shows the millimoles of benzaldehyde formed as a function of the reaction time at different temperatures (40–100 °C). From these linear plots, we calculated the reaction rates (k) for benzyl alcohol oxidation. Then, the apparent activation energy (E_a) is calculated from the slope of the linear plot of ln k *versus* $1/T$ (Figure S6B). According to the Arrhenius equation of ln k = ln $A - E_a/RT$, the activation energy was calculated to be 49.6 kJ mol^{-1}, which is lower than that reported for N-doped carbon

Table 1. Benzyl Alcohol Oxidation Catalyzed by PGc in Water[a]

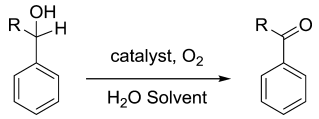

entry	catalyst	R	temp (°C)	conversion (%)	selectivity (%)
1	PGc	H	40	17.5	>99
2	PGc	H	60	24.1	>99
3	PGc	H	80	37.7	>99
4	PGc	H	100	48.4	>98.5
5[b]	PGc	H	100	41.9	>99
6	no catalyst	H	60	1.5	>99
7	rGO	H	60	7.4	>99
8	PGc-30	H	60	17.6	>99
9	PGc-180	H	60	14.4	>99
10	PGc	CH_3	80	46.5	>99
11[c]	PGc	H	60	33.4	>99
12[c]	N-doped graphene[20]	H	70	12.8[20]	100

[a]Reaction conditions: 2.0 mg alcohol, 3.0 mg catalyst, 5 mL water, oxygen balloon, 14 h reaction time. [b]Reaction conditions: 20 mg alcohol (0.2 mmol), 30 mg catalyst, 50 mL water, 1 atm O_2, 7 h reaction time. [c]Reaction conditions: 0.1 mmol alcohol, 30 mg catalyst, 80 mL water, 1 atm O_2, 10 h reaction time. Percent conversion to the alcohol and % selectivity with respect to benzaldehyde calculated using high performance liquid chromatography (HPLC). The superscripted 20 refers to numbered reference in the text.

catalysts (56.1 kJ mol^{-1})[20] and similar to Ru metal based catalysts (47.8 kJ mol^{-1}).[30,31] Moreover, unlike the N-doped carbon catalysts,[20] the PGc catalyst is able to catalyze the oxidation of secondary benzylic alcohols (1-phenethyl alcohol) with even better conversion (Table 1, entry 10). This is probably due to the unique "protruding out" structure of phosphorus atom in the graphene matrix, which is different than that of nitrogen.

It was reported that the formation of a large amount of H_2O_2 byproduct seems to be unavoidable when using noble metal based catalysts for selective oxidation of alcohols to aldehydes by molecular oxygen.[38] The generated H_2O_2 not only can possibly further react with the aldehyde product, thus leading to selectivity loss, but it could also etch the reaction equipment. Therefore, it is worth mentioning that there is no detectable H_2O_2 byproduct generated in the present reaction (Figure S7),

DOI: 10.1021/acsnano.5b07054
ACS Nano 2016, 10, 2305–2315

which is another advantage compared to transition metal catalysis.[38−40]

For industrial applications, solvent free catalytic reactions are preferred to avoid extra cost related to the use of and handling of solvents. Previously, Bielawski reported that GO is capable of catalyzing oxidation and hydration reactions in solvent free conditions. To test whether PGc can also catalyze benzyl alcohol oxidation without any solvent, neat benzyl alcohol was heated to 80 °C for 48 h in the presence of different wt % of PGc, under 1 atm of oxygen (Table 2). The % conversion with

Table 2. Optimization Experiments for Solvent Free Alcohol Oxidation Catalyzed by PGc[a]

entry	catalyst	conversion (%)	selectivity (%)	TON ($\times 10^{-2}$)
1	No catalyst	<0.1	100	NA
2	2.5 wt % PGc	2.7	>99	1.10
3	5 wt % PGc	5.1	>99	1.03
4	50 wt % PGc	21.7	98	0.44
5[b]	20 wt % PGc	27.5	96.4	1.40
6[b]	50 wt % PGc	56.1	95.7	1.14
7[b]	200 wt % PGc	90.2	96.3	0.46
8	5 wt % GO	3.7	>99	0.75
9	50 wt % GO	13.0	95	0.26
10	50 wt % re-GO[c]	4.2	95	0.09
11	50 wt % PGc-30	14.9	97	0.30
12	50 wt % PGc-180	8.4	94	0.17
13[b]	20 wt % recycled PGc[d]	22.5	96.1	1.14

[a]Reaction conditions: 50 mg catalyst, different weight of benzyl alcohol to make different wt % of catalyst, 1 atm O_2, 80 °C, 48 h. [b]Reaction was performed at 100 °C for 24 h. [c]re-GO is the catalyst, recovered from entry # 9. [d]PGc catalyst is recovered from entry # 5. Percent conversion to the alcohol and % selectivity with respect to benzaldehyde calculated using ^{1}H NMR. The turnover number (TON) was calculated as a ratio of the (mol of oxidized product)/(mass of catalyst).

PGc catalyst increases from 2.7% to 22% with the increase of the amount of catalyst loading (entries 2−4). If the reaction is performed under the same conditions, the catalytic efficiency of PGc is similar or slightly better compared to GO reported by Bielawski (entries 5−7).[18] For example, the alcohol conversion increases to 56% and 90% with 50 and 200 wt % catalyst loading, respectively, at 100 °C for 24 h (entries 5−7). The high aldehyde selectivity is largely maintained (≥96%). It was reported that at 20 wt % GO catalyst loading, a dramatic decrease in conversion efficiency from 24% to 5% was reported, indicating that a majority of the catalytic sites have been lost during the catalytic cycle. It has also been reported that the graphitic N in N-doped graphene suffered from serious stability issues.[32] To test the recyclability of the PGc, we recovered the PGc catalyst by filtration at the end of the reaction and recycled the catalyst for eight runs. Significantly, with 50 wt % PGc catalyst loading, the decrease in alcohol conversion and selectivity was not obvious (Figure 2), which is in sharp contrast to GO catalysts (Table 2, entries 9 and 10). With 20 wt % loading, the decrease in % conversion is much less compared to that of GO (Table 2, entries 5 and 13). We further compared the initial reaction rates for the fresh and the recycled PGc catalysts. As shown in Figure S8, only a trivial decrease in the reaction rate for the recycled PGc catalyst was observed. All these results suggest that the PGc catalyst has much better recyclability compared to GO.

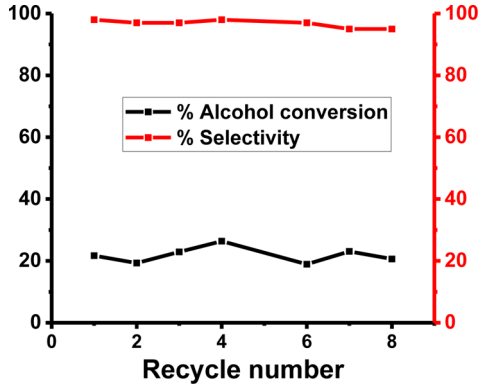

Figure 2. Recycling the PGc catalyst for benzyl alcohol oxidation. Reaction condition: 50 mg catalyst, 100 mg benzyl alcohol, 1 atm O_2, 80 °C, 48 h.

To further shed light on the role of PGc in the oxidation of benzyl alcohols, we fabricated different PGc materials. In brief, by treating the dried PGc powder with microwave irradiation for additional 30 and 180 s, we obtained different PGc materials, which we named as PGc-30 and PGc-180, respectively. The wrinkle and porous structures of these PGc materials are similar to the original PGc. Detailed treatment procedures and characterization can be found in the Supporting Information (Figures S1−S3, S5, and S9). Next, we compared the catalytic ability of these new catalysts with the original PGc in the alcohol oxidation reaction in both aqueous and solvent free conditions. As shown in Tables 1 and 2, the original PGc shows the highest alcohol conversion. The PGc-180, which was fabricated with the longest microwave irradiation time, shows the lowest conversion, followed by PGc-30 (Table 1, entries 8 and 9, and Table 2, entries 11 and 12) (*vide infra*).

The reactivity of the P-doped carbon materials for different types of alcohols was further explored using a variety of primary, secondary benzylic (1-phenethyl alcohol), alicyclic (cyclohexylmethanol) and linear (1-butanol) alcohols in solvent free conditions and the results are summarized in Table 3. We found that the PGc catalyst can catalyze secondary benzylic alcohol oxidation (23.3% conversion, entry 1) but not of aliphatic alcohols (entries 2 and 3), which is consistent with the higher reactivity of the former substrates. Very interestingly, we found that the electron donating and withdrawing properties of the functional groups attached to the aromatic ring of benzylic alcohols dramatically influenced the oxidation efficiency. 4-CH_3O-substituted benzylic alcohol reached >98% conversion and >98% selectivity to benzyl aldehyde. In contrast, the -NO_2 substituted benzyl alcohol resulted in negligible conversion (<2.5%) at the same reaction conditions. This selectivity trend has been often observed in metal-catalyzed oxidation of alcohols, but rarely in the metal free catalysis. For example, N-doped material shows no selectivity as the catalyst in the oxidation of benzylic alcohols with regard to the properties of the substituents, with electron withdrawing and donating groups showing almost the same reactivity.[20] Interestingly, the N, S, O tri-doped porous carbon materials show the opposite selectivity trend.[34]

We performed several control experiments to get insight into the PGc catalyzed alcohol oxidation reaction. It was proposed that doping with nitrogen in graphene matrix changes the electronic structure of the adjacent carbon atoms, which then react with oxygen to give peroxo-like species, which initiates the

DOI: 10.1021/acsnano.5b07054
ACS Nano 2016, 10, 2305−2315

Table 3. Catalytic Activity of PGc in the Oxidation of Different Alcohols[a]

Entry	Substrate	Product	Conversion (%)	Selectivity (%)
1[b]			23.3	95.0
2			ND	ND
3			ND	ND
4			2.2	64.1
5			52.5	94.2
6			98.9	99.9

[a]Reaction conditions: 50 mg PGc catalyst, 100 mg alcohol, 1 atm O_2, 80 °C, 48 h. [b]Reaction was run for 24 h due to acetal formation. Percent conversion and % selectivity calculated using ^{1}H NMR. ND = not determined (conversion <2.0%).

oxidation reactions.[7,15] P has the same number of valence electrons as N, and both theoretical and experimental studies have demonstrated that P-doped graphene and other graphitic carbon materials are also capable of activating molecular oxygen, which facilitates electrochemical oxygen reduction reaction (ORR).[9,23,25,41] Thus, it is reasonable to expect that the oxygen activation is the initial step in the catalytic PGc oxidation reactions, similar to N-doped graphene. If this is true, the work function of the PGc, which is closely related to its electronegativity and ionization energy, should correlate with the catalytic activity.[42] Very recently, Cheon *et al.* demonstrated that the enhanced ORR activity in doped nanocarbons is closely correlated with the variation in their nanoscale work function.[33] It was reported that among three types of nitrogen species doped into the graphene lattice, namely pyridinic N, pyrrolic N, and graphitic N, only the graphitic sp^2 N species contribute to decreasing the work function of N-doped graphene.[43] Accordingly only the graphitic sp^2 N species were established to be catalytically active centers for the aerobic oxidation reactions.[15,20] We hypothesized that PGc with lower work function should have better catalytic activity. We used PeakForce Kelvin probe force microscopy (PF-KPFM) to study the work function of the PGc fabricated with different microwave irradiation conditions (see details in Supporting Information). Unexpectedly, the PGc, which exhibited the highest activity in the oxidation of benzyl alcohol, has the highest work function (Figure 3A,B and Figure S10A,B). PGc-180, which showed the lowest reactivity, has the lowest work function (Figure 3C,D and Figure S10C,D). These unexpected results prompted us to reconsider whether O_2 is involved in the initiation step of the reaction.

For previously reported catalytic aerobic oxidation reactions, which involve oxygen activation in the first step of the reaction, the conversion decreased dramatically when the reaction was performed in an O_2 free environment.[20,32,44] To determine whether the first step of oxidation using PGc catalyst involves activation of O_2 to form peroxo like species as N-doped graphene and other graphitic carbon materials, the oxidation reaction was performed under an atmosphere of N_2, instead of O_2 (Table 4). After 48 h of reaction at 80 °C, 18% alcohol

Table 4. Recycling the PGc Catalyst in Benzyl Alcohol Oxidation in the Presence of Different Environment[a]

entry	catalyst	oxidant	conversion (%)	selectivity (%)
1	PGc	N_2	17.6	99.8
2	PGc-second cycle	N_2	3.2	99.9
3	PGc-third cycle	O_2	22.7	94.0

[a]Reaction conditions: 50 mg PGc catalyst, 100 mg of alcohol, 1 atm oxidant, 80 °C, 48 h. Percent conversion to the alcohol and % selectivity with respect to benzaldehyde calculated using ^{1}H NMR.

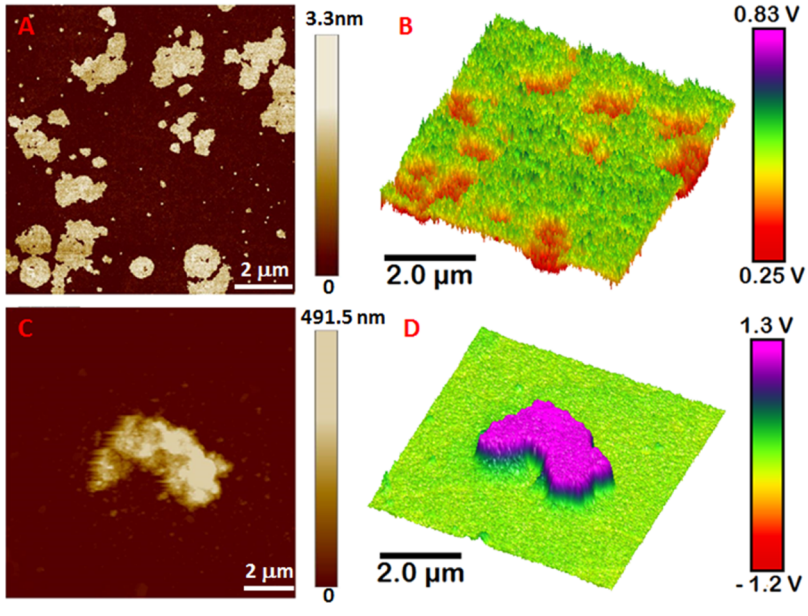

Figure 3. (A and C) Topography and (B and D) PF-KPFM images of PGc and PGc-180 catalysts, respectively.

DOI: 10.1021/acsnano.5b07054
ACS Nano 2016, 10, 2305−2315

conversion was found, which is just slightly lower than that under 1 atm O_2 (23% conversion), indicating that some functional groups on PGc are directly involved in the alcohol oxidation reaction without the requirement for external O_2. Very interestingly, we found that the alcohol conversion decreased significantly (3%) after the same PGc catalyst was cleaned under N_2 environment, and reused for the catalytic reaction under N_2 environment. However, % alcohol conversion recovered back to 23% when the PGc catalyst was recycled for the third time, but the reaction was performed in the presence of 1 atm O_2. Altogether, these results suggest that O_2 does not directly react with the substrate, yet it is needed to regenerate the functional groups/active sites on PGc for the catalytic oxidation. This is very different from GO, N doped, and N, B co-doped carbon catalysts.[12,15,18,20]

To understand if free radical intermediates are involved during the PGc catalyzed oxidation, we performed the benzyl alcohol oxidation reaction (PGc catalyst, 1 atm O_2) in the presence of butylated hydroxytoluene (BHT, 20 wt %), a known free radical quencher (Table 5). After 24 h, analysis of the reaction mixture revealed that the same conversion and selectivity were reached, suggesting that the presence of BHT did not inhibit the reaction. This result is very different from GO catalyzed aerobic oxidation of alcohols in which a dramatic decrease of the conversion efficiency was observed upon addition of BHT, from 24 to 5%.[18] This result is also different from those of N and N, B co-doped graphene-like materials in aerobic oxidation of benzylic compounds.[12] In these cases, it was found that including BHT in the reaction mixture completely blocked the benzylic oxidation.

Table 5. Benzyl Alcohol Oxidation in the Presence of Radical Quencher[a]

entry	catalyst	radical inhibitor	conversion (%)	selectivity (%)
1	50 wt % PGc	-	21.2	>99
2	50 wt % PGc	BHT	22.2	98.6

[a]Reaction conditions: 50 mg PGc catalyst, 100 mg of alcohol, 0.3 mL acetonitrile, 1 atm O_2, 80 °C, 24 h. Butylated hydroxytoluene (BHT, 0.1 mmol) is added in entry 2 for controlled reaction. Percentage conversion for alcohols and % selectivity to benzaldehyde is calculated using ^{1}H NMR.

To find out the possible active sites on PGc catalysts, the detailed chemical composition and the bonding configuration of phosphorus atoms in the P-doped carbon materials were studied by X-ray photoelectron spectroscopy (XPS) and Fourier transform infrared spectroscopy (FT-IR). The XPS spectra showed that the PGc contains mainly three elements, C, O, and P, with atomic % of 74.0%, 21.2%, and 4.9%, respectively (Figure S1, Table S1). The PGc material was also analyzed by X-ray fluorescence spectroscopy (XRF) to calculate % P in the bulk material and found to be ~3 atom % or ~9 wt % (Figure S11). To determine the chemical bond configuration of P present in the PGc, both the high resolution P 2p peak and O 1s peak were deconvoluted (Figure 4). It is worth mentioning that the peak deconvolution and assignment are discussed in many papers.[45] It is widely accepted that the P 2p peaks at higher binding energy (>132 eV) are P-containing functional groups associated with −C−O−C, −OH, or =O, and the peak position shifts to higher binding energy as the oxidation state of P becomes higher.[45] For the sake of simplicity, in this work the P 2p peak was deconvoluted into two components. According to the most comprehensively explained results in the literature, the peak centered at 132.5 eV was assigned to P−C (28.4%), which suggested that P atoms are indeed incorporated into the carbon lattice. The peak at 134.7 eV was assigned to P−O (~71.6%) bonds, which represents all the P-containing functional groups associated with O.

The deconvolution of O 1s peak demonstrated that 62.6% of the total oxygen is in the form of C−OH/P−OH, 16.0% C−O−P/C−O−C, 10.5% C=O/P=O and 11.0% in the form of adsorbed water/COOH functionality. It is difficult to differentiate between C=O and P=O, C−O−P and C−O−C, and P−OH and C−OH due to their very close binding energy. To solve these problems, the PGc was further characterized with FT-IR spectroscopy (Figure 5). The spectra of GO and rGO is also displayed for comparison. Unlike GO, PGc does not show the strong peaks at 1719 cm^{-1}(C=O stretching), 1410 cm^{-1} (C−O stretching in carboxylic acid or carboxylate) and 1230 cm^{-1}(C−OH/C−O−C stretching).[46,47] However, the spectra clearly shows several peaks at 1166, 1131 (shoulder), 1035, 900 cm^{-1} (shoulder), and several weaker peaks (750−663 cm^{-1}), which can be assigned to P=O stretching, P−C of P-aromatic stretching, P−O−C, P−OH, and P−C.[48,49] These results demonstrate that mainly P=O, instead of C=O, exists in the PGc, C−O−C groups are below the detection limit, and the majority of −OH present in PGc is directly bonded to P with abundant P−OH functionalities. Moreover, since the atomic O/P ratio is ~4 from XPS studies, some P atoms possibly connect with two or more oxygen containing functionalities, such as OH groups as schematically proposed in Scheme 1.

To study which functionality is important for the observed catalytic activities of PGc, we carefully studied the functional groups of PGc-30 and PGc-180 materials. The XPS spectra showed that both catalysts, PGc-30 and PGc-180, have similar amount of % O (13.52, 13.60% respectively), which is lower than PGc (21.17% O) (Table S1). Furthermore, XPS and FT-IR analysis showed that they (PGc-30 and PGc-180) contain similar amounts of C−O−P and P=O groups, while PGc-180 has the lowest content of P−OH functionalities as per O 1s XPS peak analysis of PGc-180 catalyst (Figure 4 and Figure S12 and Table S3). Note that PGc-180 also exhibited the lowest alcohol conversion, followed by PGc-30 and PGc, respectively, suggesting that the P−OH functional groups on PGc are likely to play an important role in the oxidation. On the other hand, we have also performed benzyl alcohol oxidation reaction in the presence of molecules containing P=O and P−OH functional groups, such as phytic acid and phosphorous acid. The reaction does not proceed, which indicates the importance of the graphitic regions on the PGc material for aromatic substrate interaction.

On the basis of all the experimental results described above, we have concluded the following important points regarding the catalytic mechanism of alcohol oxidation by PGc. (1) The PGc with higher work function shows higher catalytic activity, which is opposite to that of N-doped graphene and other graphitic carbon materials. (2) Molecular oxygen is not involved in the first step of the reaction, which is also different from N-doped graphene. However, the presence of oxygen is critical for regenerating the active sites on the PGc catalysts. (3) The coexistence of P=O, P−OH functionalities along with the graphitic regions on PGc play a pivotal role in the catalytic alcohol oxidation reaction. (4) A radical inhibitor, BHT, does not inhibit the oxidation reaction. (5) There are no detectable

DOI: 10.1021/acsnano.5b07054
ACS Nano 2016, 10, 2305−2315

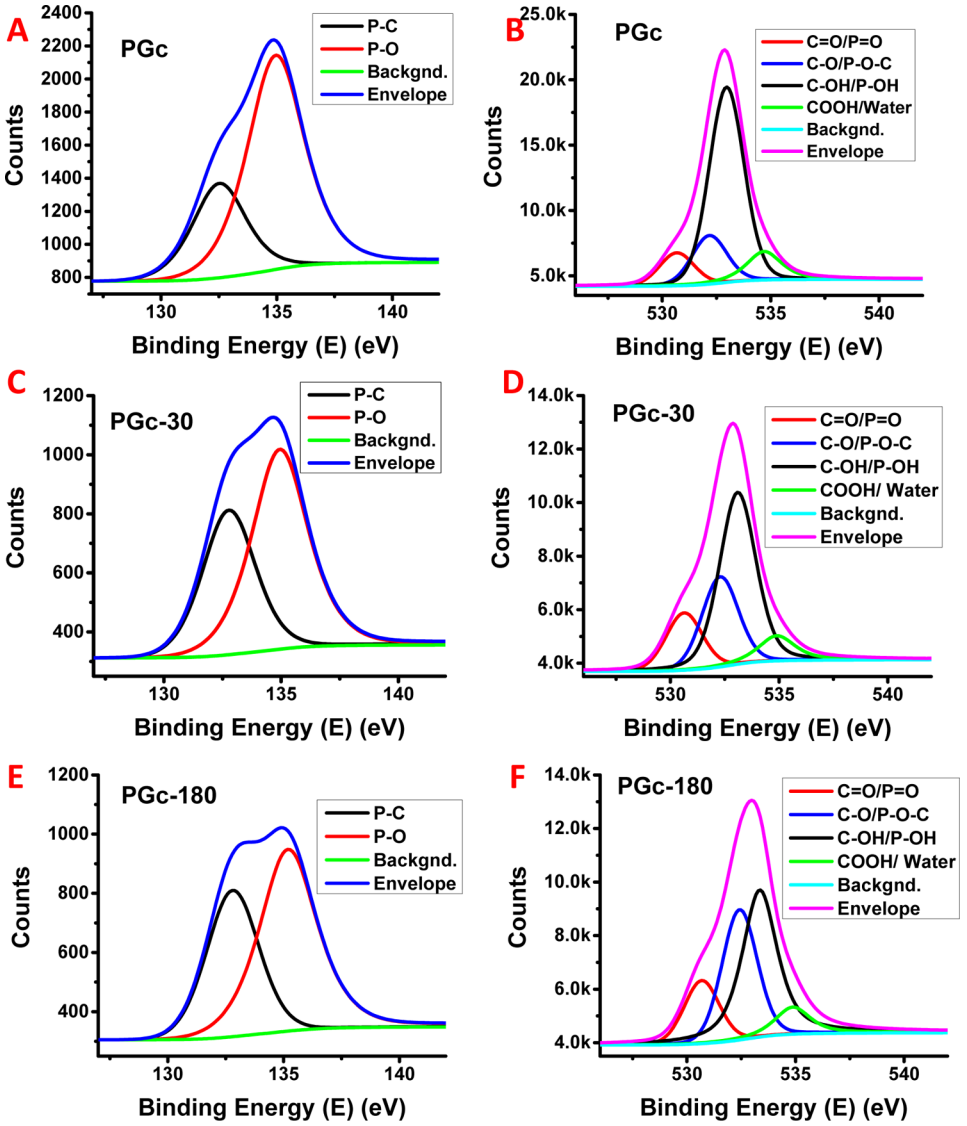

Figure 4. P 2p (A, C, E) and O 1s (B, D, F) peak deconvolution of different PGc catalysts, PGc, PGc-30, and PGc-180, respectively.

H_2O_2 as byproduct generated during the reaction (Figure S7). (6) In addition, the reaction is associated with loss of water when reaction was performed under oxygen as demonstrated by the presence of water peak in ^{1}H NMR spectroscopy of the final product mixture (Figure S13).

On the basis of these findings and previous reports using P_2O_5 to accelerate the oxidation of alcohols[50] and carbohydrates,[51] and especially, a recent finding suggesting the importance of ketonic O in catalysis of benzylic alcohol oxidation,[52] we propose the following mechanism as shown in Scheme 2 where primary benzyl alcohol is used as an example. In the first step of catalysis, condensation between the alcohol and P═O moieties on PGc takes place, and an alcoholate intermediate is formed. The condensation is likely facilitated by the interaction of the alcohol with the PGc surface by $\pi-\pi$ interactions with the graphitic domains and hydrogen bonding with the polar groups (such as P−OH). In the second step of the reaction, a rate determining H transfer takes place, possibly through a cyclic transition state. This step is supported by the linear Hammett correlation in the oxidation of 4-substituted benzylic alcohols by PGc (Figure S14, plot of log k *vs* σ gives a ρ value of −1.50, R^2 = 0.98, independent rates), indicating buildup of a positive charge in the transition state. The proton transfer step is facilitated by P−OH moieties on PGc surface. Notably, the observed Hammett rho value is in the range reported for oxidation of benzylic alcohols using pyridinium chlorochromate (−1.4 to −1.7)[53−55] and much higher than that reported for oxidation of benzylic alcohols *via* the radical mechanism (−0.4).[56−58] It is likely that the presence of hydrogen bonding between the substrate and the PGc polar groups stabilizes the transition state, enabling the alcohol oxidation in the close proximity to the material surface. The aldehyde product and a water molecule are released simultaneously. Next, the generated P(III) groups on PGc react with molecular oxygen to regenerate the P(V) centers for further reactions, thus completing the catalytic cycle (Scheme 2). The PGc catalyst after the reaction was characterized *via* FT-IR. The peaks at 1166 cm^{-1} (P═O), 1035 cm^{-1} (P−O/C-O), 900 cm^{-1} (shoulder, P−OH) have similar intensities as the fresh PGc catalyst (Figure S15), indicating that the catalytic sites are largely being regenerated during the reaction. Moreover, recently, Hasegawa *et al.* demonstrated that the reduced form of P functionalities, which were initially introduced into the carbon matrix of graphene, were unstable

DOI: 10.1021/acsnano.5b07054
ACS Nano 2016, 10, 2305−2315

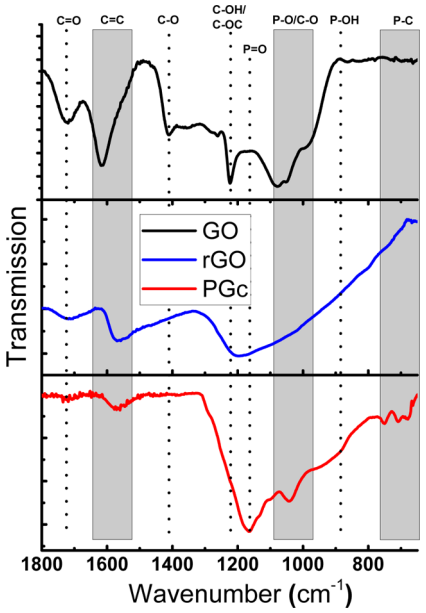

Figure 5. FT-IR spectra comparison of PGc with GO and rGO catalysts.

Scheme 2. Proposed Mechanism of Benzyl Alcohol Oxidation Catalyzed by PGc in the Presence of Oxygen As an Oxidant

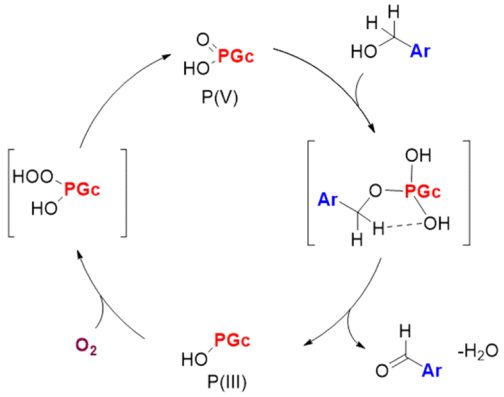

and gradually oxidized and/or hydrolyzed by O_2 and humidity at ambient conditions and room temperature, leading to the formation of oxidized P-containing functional groups.[45] This study also soundly supports the hypothesis that P−OH/P═O functionalities of PGc can be readily regenerated.

The excellent recyclability is one of the key advantages of PGc compared to the GO based catalysts. Boukhvalov *et al.* applied density functional theory (DFT) calculations on GO to reveal that the partially reduced catalyst, which is different from the inert graphite or pristine graphene, can be recharged by molecular oxygen, allowing for catalyst turnover.[35] However, experimentally, it was reported that after the reaction, the GO catalyst was transformed to rGO, especially at relatively low catalyst loading such as 20 wt %. The recovered rGO has similar electronic properties as rGO intentionally prepared by other methods, indicating that regeneration of the active sites under the reaction conditions did not occur fast enough.[18]

CONCLUSIONS

In summary, we have reported an extremely simple, energy effective, and scalable approach to rapidly fabricate P-doped carbon materials with controlled P bond configuration. For the first time, we demonstrated that the P-doped carbon materials can be used as a selective metal free catalyst for aerobic oxidation of benzylic alcohols with >98% selectivity to benzaldehydes. The P bond configuration influences the work function of P-doped carbon materials. However, in sharp contrast to N-doped graphene and other graphitic carbon materials, the PGc material with higher work function shows high activity in catalytic aerobic oxidation. On the basis of our extensive experimental studies, a unique catalytic mechanism seems to be operating when PGc catalysts are used, which is different from both GO and N-doped graphene obtained by high temperature nitrification. While the apparent conversion is similar to GO, the key advantage compared to GO is that this catalyst, even with low catalyst loading, can be reused multiple times with simple filtration without losing its catalytic activity. Compared to the N-doped graphene, not only the conversion increased 3 times without losing selectivity, this catalyst also shows no steric effect as both primary and secondary alcohol can be converted with similar conversion efficiency. Finally, while our study focused on alcohol oxidation, it is also worthy to mention that phosphate functionalized carbon materials have been used for acidic catalytic reactions,[59] to increase the selectivity of the oxidative dehydration reactions,[60] and widen the electrochemical potential window in high capacitance applications.[61] All these are due to the different P bond configuration in these carbon materials, which in turn demonstrated the rich P chemistry can be tailored to fit different applications. Importantly, we have already demonstrated that P carbon materials co-doped with other heteroatoms, such as N, B, S, and Si, can also be fabricated by this microwave assisted approach by simply adding a suitable dopant precursor into the reactor.[62] Altogether, combining these facts with the capability of co-doping with other heteroatoms *via* this simple microwave assisted approach, it is reasonable to predict that tailored carbon materials can be designed and quickly fabricated to develop more efficient and metal free carbon based catalysts for wide range of reactions and other sustainable applications.

METHODS

The synthetic procedure for all the catalysts (PGc, PGc-30 and PGc-180 catalysts), GO, rGO is described in detail in the Supporting Information. In brief, PGc was synthesized by heating the phytic acid (Sigma-Aldrich, 50 w/w% in water, 1 mL) in domestic microwave oven (1100W, Sanyo-EM-S9515W, 2.45 GHz) for 40 s. PGc-30 and PGc-180 were synthesized by heating the PGc powder into domestic microwave for 30 and 180 s, respectively. GO was synthesized by modified hummers method with slight modification.[46] The rGO was synthesized by heating (500 mg of GO) in a microwave (CEM discover SP) at 300 W for 40 s. For the catalytic alcohol oxidation reaction, the catalyst, oxidant and solvent (if it mentioned in table footnote) are mixed and sealed in desired atmosphere and heated in oil bath at predetermined temperature and time (see detailed description in Supporting Information). After completion of the reaction, the reaction mixture was filtered *via* 0.02 μm syringe filter and analyzed by HPLC or ^{1}H NMR spectroscopy (see Supporting Information for more detail).

Material Characterization. PF-KPFM measurements of the PGc and PGc-180 catalysts were conducted using a Dimension ICON AFM setup inside a nitrogen-filled glovebox where both H_2O and O_2 level

DOI: 10.1021/acsnano.5b07054
ACS Nano 2016, 10, 2305−2315

were below 0.1 ppm. The tips used were PFQNE-AL (Bruker AFM Probes), composed of a silicon nitride cantilever with a sharp silicon tip. The morphology of graphene samples were studied using the scanning electron microscopy (SEM, Hitachi S-4800). The sample for SEM was prepared by directly adding the powder sample on a conductive carbon tape. X-ray photoelectron spectroscopy (XPS) characterization was performed after depositing a layer of the catalyst to be studied onto a Si substrate. The thickness of the film on the substrates was roughly 30−50 nm. XPS spectra were acquired using a Thermo Scientific K-Alpha system with a monochromatic Al Kα X-ray source ($h\nu$ = 1486.7 eV). For data analysis, Smart background subtraction was performed, and the spectra were fit with Gaussian/Lorentzian peaks using a minimum deviation curve fitting method (part of the Avantage software package). The surface composition of each species was determined by the integrated peak areas and the Scofield sensitivity factor provided by the Avantage software. The FT-IR spectra of the samples (thin films deposited on ZnSe windows) were acquired with a Thermo-Nicolet 6700 spectrometer (Thermo-Electron Corp., Madison, WI), using a sample shuttle and a mercury−cadmium-telluride (MCT) detector. Four blocks of 128 scans each were coadded with 4 cm^{-1} spectral resolution and two levels of zero-filling so that data was encoded every 1 cm^{-1}. Thermo gravimetric analyses (TGA) of the PGc samples were performed on a TGA instrument (TA Instruments, Discovery TGA) from 40 to 900 °C at 5 °C/min under N_2 flow (20 mL/min). The Raman spectra of the PGc and other samples (deposited on Anodisc membrane) were collected using Raman Microscope (Confocal) − Wi-Tec, Alpha 3000R with an excitation laser at 785 nm. The X-ray fluorescence spectroscopic (XRF) measurement was carried out using Horiba XGT-1000WR with high purity Si detector. (See Supporting Information for more detailed description about the sample preparation and characterization for all the instrumental analysis.)

ASSOCIATED CONTENT

Supporting Information

The Supporting Information is available free of charge on the ACS Publications website at DOI: 10.1021/acsnano.5b07054.

Fabrication and characterization of catalysts, experimental procedures and compound characterization data (PDF)

AUTHOR INFORMATION

Corresponding Authors

*E-mail: huixinhe@ rutgers.edu.
*E-mail: michal.szostak@rutgers.edu.

Notes

The authors declare no competing financial interest.

ACKNOWLEDGMENTS

Financial support was provided the National Science Foundation (CBET 1438493 and DMR 1507812). The Bruker 500 MHz spectrometer used in this study was supported by the NSF-MRI Grant (CHE-1229030). Work function studies with Kelvin Probe Microscope were supported by NSF MRI 1429062. The authors are grateful to Dr. Kristina Keating from Department of Earth and Environmental Sciences, Rutgers University—Newark, for help in BET measurement of PGc catalyst. The authors are grateful to Dr. Qihong Zhang from Department of Chemistry, Rutgers University—Newark, for her help in Raman measurements of PGc catalyst.

REFERENCES

(1) Navalon, S.; Dhakshinamoorthy, A.; Alvaro, M.; Garcia, H. Carbocatalysis by Graphene-Based Materials. *Chem. Rev.* **2014**, *114*, 6179−6212.

(2) Su, C.; Loh, K. P. Carbocatalysts: Graphene Oxide and Its Derivatives. *Acc. Chem. Res.* **2013**, *46*, 2275−2285.

(3) Fan, X.; Zhang, G.; Zhang, F. Multiple Roles of Graphene in Heterogeneous Catalysis. *Chem. Soc. Rev.* **2015**, *44*, 3023−3035.

(4) Hu, H. W.; Xin, J. H.; Hu, H.; Wang, X. W.; Kong, Y. Y. Metal-Free Graphene-Based Catalyst-Insight into the Catalytic Activity: A Short Review. *Appl. Catal., A* **2015**, *492*, 1−9.

(5) Su, D. S.; Perathoner, S.; Centi, G. Nanocarbons for the Development of Advanced Catalysts. *Chem. Rev.* **2013**, *113*, 5782−5816.

(6) Kong, X. K.; Chen, C. L.; Chen, Q. W. Doped Graphene for Metal-Free Catalysis. *Chem. Soc. Rev.* **2014**, *43*, 2841−2857.

(7) Gong, K.; Du, F.; Xia, Z.; Durstock, M.; Dai, L. Nitrogen-Doped Carbon Nanotube Arrays with High Electrocatalytic Activity for Oxygen Reduction. *Science* **2009**, *323*, 760−764.

(8) Jiao, Y.; Zheng, Y.; Jaroniec, M.; Qiao, S. Z. Origin of the Electrocatalytic Oxygen Reduction Activity of Graphene-Based Catalysts: A Roadmap to Achieve the Best Performance. *J. Am. Chem. Soc.* **2014**, *136*, 4394−4403.

(9) Zhang, C.; Mahmood, N.; Yin, H.; Liu, F.; Hou, Y. Synthesis of Phosphorus-Doped Graphene and Its Multifunctional Applications for Oxygen Reduction Reaction and Lithium Ion Batteries. *Adv. Mater.* **2013**, *25*, 4932−4937.

(10) Patel, M.; Feng, W.; Savaram, K.; Khoshi, M. R.; Huang, R.; Sun, J.; Rabie, E.; Flach, C.; Mendelsohn, R.; Garfunkel, E.; He, H. Microwave Enabled One-Pot, One-Step Fabrication and Nitrogen Doping of Holey Graphene Oxide for Catalytic Applications. *Small* **2015**, *11*, 3358−3368.

(11) Su, C.; Acik, M.; Takai, K.; Lu, J.; Hao, S. J.; Zheng, Y.; Wu, P.; Bao, Q.; Enoki, T.; Chabal, Y. J.; Loh, K. P. Probing the Catalytic Activity of Porous Graphene Oxide and the Origin of This Behaviour. *Nat. Commun.* **2012**, *3*, 1298.

(12) Dhakshinamoorthy, A.; Primo, A.; Concepcion, P.; Alvaro, M.; Garcia, H. Doped Graphene as a Metal-Free Carbocatalyst for the Selective Aerobic Oxidation of Benzylic Hydrocarbons, Cyclooctane and Styrene. *Chem. - Eur. J.* **2013**, *19*, 7547−7554.

(13) Li, X. H.; Chen, J. S.; Wang, X.; Sun, J.; Antonietti, M. Metal-Free Activation of Dioxygen by Graphene/G-C3n4 Nanocomposites: Functional Dyads for Selective Oxidation of Saturated Hydrocarbons. *J. Am. Chem. Soc.* **2011**, *133*, 8074−8077.

(14) Li, X. H.; Antonietti, M. Polycondensation of Boron- and Nitrogen-Codoped Holey Graphene Monoliths from Molecules: Carbocatalysts for Selective Oxidation. *Angew. Chem., Int. Ed.* **2013**, *52*, 4572−4576.

(15) Gao, Y.; Hu, G.; Zhong, J.; Shi, Z.; Zhu, Y.; Su, D. S.; Wang, J.; Bao, X.; Ma, D. Nitrogen-Doped Sp2-Hybridized Carbon as a Superior Catalyst for Selective Oxidation. *Angew. Chem., Int. Ed.* **2013**, *52*, 2109−2113.

(16) Jia, H. P.; Dreyer, D. R.; Bielawski, C. W. Graphite Oxide as an Auto-Tandem Oxidation-Hydration-Aldol Coupling Catalyst. *Adv. Synth. Catal.* **2011**, *353*, 528−532.

(17) Jia, H. P.; Dreyer, D. R.; Bielawski, C. W. C-H Oxidation Using Graphite Oxide. *Tetrahedron* **2011**, *67*, 4431−4434.

(18) Dreyer, D. R.; Jia, H. P.; Bielawski, C. W. Graphene Oxide: A Convenient Carbocatalyst for Facilitating Oxidation and Hydration Reactions. *Angew. Chem., Int. Ed.* **2010**, *49*, 6813−6816.

(19) Li, W. J.; Gao, Y. J.; Chen, W. L.; Tang, P.; Li, W. Z.; Shi, Z. J.; Su, D. S.; Wang, J. G.; Ma, D. Catalytic Epoxidation Reaction over N-Containing sp^2 Carbon Catalysts. *ACS Catal.* **2014**, *4*, 1261−1266.

(20) Long, J. L.; Xie, X. Q.; Xu, J.; Gu, Q.; Chen, L. M.; Wang, X. X. Nitrogen-Doped Graphene Nanosheets as Metal-Free Catalysts for Aerobic Selective Oxidation of Benzylic Alcohols. *ACS Catal.* **2012**, *2*, 622−631.

(21) Van Khai, T.; Na, H. G.; Kwak, D. S.; Kwon, Y. J.; Ham, H.; Shim, K. B.; Kim, H. W. Significant Enhancement of Blue Emission and Electrical Conductivity of N-Doped Graphene. *J. Mater. Chem.* **2012**, *22*, 17992−18003.

DOI: 10.1021/acsnano.5b07054
ACS Nano 2016, 10, 2305−2315

(22) Wang, X.; Sun, G.; Routh, P.; Kim, D. H.; Huang, W.; Chen, P. Heteroatom-Doped Graphene Materials: Syntheses, Properties and Applications. *Chem. Soc. Rev.* **2014**, *43*, 7067−7098.
(23) Yang, D. S.; Bhattacharjya, D.; Inamdar, S.; Park, J.; Yu, J. S. Phosphorus-Doped Ordered Mesoporous Carbons with Different Lengths as Efficient Metal-Free Electrocatalysts for Oxygen Reduction Reaction in Alkaline Media. *J. Am. Chem. Soc.* **2012**, *134*, 16127−16130.
(24) Some, S.; Kim, J.; Lee, K.; Kulkarni, A.; Yoon, Y.; Lee, S.; Kim, T.; Lee, H. Highly Air-Stable Phosphorus-Doped N-Type Graphene Field-Effect Transistors. *Adv. Mater.* **2012**, *24*, 5481−5486.
(25) Liu, Z. W.; Peng, F.; Wang, H. J.; Yu, H.; Zheng, W. X.; Yang, J. Phosphorus-Doped Graphite Layers with High Electrocatalytic Activity for the O_2 Reduction in an Alkaline Medium. *Angew. Chem., Int. Ed.* **2011**, *50*, 3257−3261.
(26) Latorre-Sanchez, M.; Primo, A.; Garcia, H. P-Doped Graphene Obtained by Pyrolysis of Modified Alginate as a Photocatalyst for Hydrogen Generation from Water-Methanol Mixtures. *Angew. Chem., Int. Ed.* **2013**, *52*, 11813−11816.
(27) Zhang, X. L.; Lu, Z. S.; Fu, Z. M.; Tang, Y. A.; Ma, D. W.; Yang, Z. X. The Mechanisms of Oxygen Reduction Reaction on Phosphorus Doped Graphene: A First-Principles Study. *J. Power Sources* **2015**, *276*, 222−229.
(28) Wang, H. M.; Wang, H. X.; Chen, Y.; Liu, Y. J.; Zhao, J. X.; Cai, Q. H.; Wang, X. Z. Phosphorus-Doped Graphene and (8,0) Carbon Nanotube: Structural, Electronic, Magnetic Properties, and Chemical Reactivity. *Appl. Surf. Sci.* **2013**, *273*, 302−309.
(29) Liu, Z. W.; Peng, F.; Wang, H. J.; Yu, H.; Zheng, W. X.; Wei, X. Y. Preparation of Phosphorus-Doped Carbon Nanospheres and Their Electrocatalytic Performance for O_2 Reduction. *J. Nat. Gas Chem.* **2012**, *21*, 257−264.
(30) Yamaguchi, K.; Mizuno, N. Scope, Kinetics, and Mechanistic Aspects of Aerobic Oxidations Catalyzed by Ruthenium Supported on Alumina. *Chem. - Eur. J.* **2003**, *9*, 4353−4361.
(31) Dijksman, A.; Marino-Gonzalez, A.; MairataiPayeras, A.; Arends, I. W.; Sheldon, R. A. Efficient and Selective Aerobic Oxidation of Alcohols into Aldehydes and Ketones Using Ruthenium/Tempo as the Catalytic System. *J. Am. Chem. Soc.* **2001**, *123*, 6826−6833.
(32) Watanabe, H.; Asano, S.; Fujita, S.; Yoshida, H.; Arai, M. Nitrogen-Doped, Metal-Free Activated Carbon Catalysts for Aerobic Oxidation of Alcohols. *ACS Catal.* **2015**, *5*, 2886−2894.
(33) Cheon, J. Y.; Kim, J. H.; Goddeti, K. C.; Park, J. Y.; Joo, S. H. Intrinsic Relationship between Enhanced Oxygen Reduction Reaction Activity and Nanoscale Work Function of Doped Carbons. *J. Am. Chem. Soc.* **2014**, *136*, 8875−8878.
(34) Meng, Y. Y.; Voiry, D.; Goswami, A.; Zou, X. X.; Huang, X. X.; Chhowalla, M.; Liu, Z. W.; Asefa, T. N-, O-, and S-Tridoped Nanoporous Carbons as Selective Catalysts for Oxygen Reduction and Alcohol Oxidation Reactions. *J. Am. Chem. Soc.* **2014**, *136*, 13554−13557.
(35) Boukhvalov, D. W.; Dreyer, D. R.; Bielawski, C. W.; Son, Y. W. A Computational Investigation of the Catalytic Properties of Graphene Oxide: Exploring Mechanisms by Using DFT Methods. *ChemCatChem* **2012**, *4*, 1844−1849.
(36) Ramasahayam, S. K.; Nasini, U. B.; Bairi, V.; Shaikh, A. U.; Viswanathan, T. Microwave Assisted Synthesis and Characterization of Silicon and Phosphorous Co-Doped Carbon as an Electrocatalyst for Oxygen Reduction Reaction. *RSC Adv.* **2014**, *4*, 6306−6313.
(37) Ramasahayam, S. K.; Nasini, U. B.; Shaikh, A. U.; Viswanathan, T. Novel Tannin-Based Si, P Co-Doped Carbon for Supercapacitor Applications. *J. Power Sources* **2015**, *275*, 835−844.
(38) Enache, D. I.; Edwards, J. K.; Landon, P.; Solsona-Espriu, B.; Carley, A. F.; Herzing, A. A.; Watanabe, M.; Kiely, C. J.; Knight, D. W.; Hutchings, G. J. Solvent-Free Oxidation of Primary Alcohols to Aldehydes Using Au-Pd/TiO_2 Catalysts. *Science* **2006**, *311*, 362−365.
(39) Liu, H. L.; Liu, Y. L.; Li, Y. W.; Tang, Z. Y.; Jiang, H. F. Metal-Organic Framework Supported Gold Nanoparticles as a Highly Active Heterogeneous Catalyst for Aerobic Oxidation of Alcohols. *J. Phys. Chem. C* **2010**, *114*, 13362−13369.
(40) Zhu, J.; Wang, P. C.; Lu, M. Selective Oxidation of Benzyl Alcohol under Solvent-Free Condition with Gold Nanoparticles Encapsulated in Metal-Organic Framework. *Appl. Catal., A* **2014**, *477*, 125−131.
(41) Liu, Z. W.; Peng, F.; Wang, H. J.; Yu, H.; Tan, J.; Zhu, L. L. Novel Phosphorus-Doped Multiwalled Nanotubes with High Electrocatalytic Activity for O_2 Reduction in Alkaline Medium. *Catal. Commun.* **2011**, *16*, 35−38.
(42) Gholizadeh, R.; Yu, Y. X. Work Functions of Pristine and Heteroatom-Doped Graphenes under Different External Electric Fields: An *ab initio* DFT Study. *J. Phys. Chem. C* **2014**, *118*, 28274−28282.
(43) Schiros, T.; Nordlund, D.; Palova, L.; Prezzi, D.; Zhao, L.; Kim, K. S.; Wurstbauer, U.; Gutierrez, C.; Delongchamp, D.; Jaye, C.; Fischer, D.; Ogasawara, H.; Pettersson, L. G.; Reichman, D. R.; Kim, P.; Hybertsen, M. S.; Pasupathy, A. N. Connecting Dopant Bond Type with Electronic Structure in N-Doped Graphene. *Nano Lett.* **2012**, *12*, 4025−4031.
(44) Dreyer, D. R.; Jia, H. P.; Bielawski, C. W. Graphene Oxide: A Convenient Carbocatalyst for Facilitating Oxidation and Hydration Reactions. *Angew. Chem.* **2010**, *122*, 6965−6968.
(45) Hasegawa, G.; Deguchi, T.; Kanamori, K.; Kobayashi, Y.; Kageyama, H.; Abe, T.; Nakanishi, K. High-Level Doping of Nitrogen, Phosphorus, and Sulfur into Activated Carbon Monoliths and Their Electrochemical Capacitances. *Chem. Mater.* **2015**, *27*, 4703−4712.
(46) Hu, F.; Patel, M.; Luo, F.; Flach, C.; Mendelsohn, R.; Garfunkel, E.; He, H.; Szostak, M. Graphene-Catalyzed Direct Friedel-Crafts Alkylation Reactions: Mechanism, Selectivity, and Synthetic Utility. *J. Am. Chem. Soc.* **2015**, *137*, 14473−14480.
(47) Marcano, D. C.; Kosynkin, D. V.; Berlin, J. M.; Sinitskii, A.; Sun, Z.; Slesarev, A.; Alemany, L. B.; Lu, W.; Tour, J. M. Improved Synthesis of Graphene Oxide. *ACS Nano* **2010**, *4*, 4806−4814.
(48) Puziy, A. M.; Poddubnaya, O. I.; Martinez-Alonso, A.; Suarez-Garcia, F.; Tascon, J. M. D. Surface Chemistry of Phosphorus-Containing Carbons of Lignocellulosic Origin. *Carbon* **2005**, *43*, 2857−2868.
(49) Puziy, A. M.; Poddubnaya, O. I.; Ziatdinov, A. M. On the Chemical Structure of Phosphorus Compounds in Phosphoric Acid-Activated Carbon. *Appl. Surf. Sci.* **2006**, *252*, 8036−8038.
(50) Khazaei, A.; Rad, M. N. S.; Borazjani, M. K.; Saednia, S.; Borazjani, M. K.; Golbaghi, M.; Behrouz, S. Highly Efficient Etherification and Oxidation of Aromatic Alcohols Using Supported and Unsupported Phosphorus Pentoxide as a Heterogeneous Reagent. *Synth. Commun.* **2011**, *41*, 1544−1553.
(51) Onodera, K.; Hirano, S.; Kashimura, N. Oxidation of Carbohydrates with Dimethyl Sulfoxide Containing Phosphorus Pentoxide. *J. Am. Chem. Soc.* **1965**, *87*, 4651−4652.
(52) Jeyaraj, V. S.; Kamaraj, M.; Subramanian, V. Generalized Reaction Mechanism for the Selective Aerobic Oxidation of Aryl and Alkyl Alcohols over Nitrogen-Doped Graphene. *J. Phys. Chem. C* **2015**, *119*, 26438−26450.
(53) Banerji, K. K. Oxidation of Substituted Benzyl Alcohols by Pyridinium Fluorochromate - a Kinetic-Study. *J. Org. Chem.* **1988**, *53*, 2154−2159.
(54) Stewart, R.; Lee, D. G. The Chromic Acid Oxidation of Aryl Trifluoromethyl Alcohols: Isotope and Substituent Effects. *Can. J. Chem.* **1964**, *42*, 439−446.
(55) Banerji, K. K. Kinetics and Mechanism of the Oxidation of Substituted Benzyl Alcohols by Pyridinium Chlorochromate. *J. Chem. Soc., Perkin Trans. 2* **1978**, 639−641.
(56) De Nooy, A. E.; Besemer, A. C.; van Bekkum, H. On the Use of Stable Organic Nitroxyl Radicals for the Oxidation of Primary and Secondary Alcohols. *Synthesis* **1996**, *1996*, 1153−1176.
(57) Minisci, F.; Recupero, F.; Cecchetto, A.; Gambarotti, C.; Punta, C.; Faletti, R.; Paganelli, R.; Pedulli, G. F. Mechanisms of the Aerobic Oxidation of Alcohols to Aldehydes and Ketones, Catalysed under Mild Conditions by Persistent and Non-Persistent Nitroxyl Radicals and Transition Metal Salts− Polar, Enthalpic, and Captodative Effects. *Eur. J. Org. Chem.* **2004**, *2004*, 109−119.

DOI: 10.1021/acsnano.5b07054
ACS Nano 2016, 10, 2305−2315

(58) Koshino, N.; Saha, B.; Espenson, J. H. Kinetic Study of the Phthalimide N-Oxyl Radical in Acetic Acid. Hydrogen Abstraction from Substituted Toluenes, Benzaldehydes, and Benzyl Alcohols. *J. Org. Chem.* **2003**, *68*, 9364−9370.
(59) Villa, A.; Schiavoni, M.; Fulvio, P. F.; Mahurin, S. M.; Dai, S.; Mayes, R. T.; Veith, G. M.; Prati, L. Phosphorylated Mesoporous Carbon as Effective Catalyst for the Selective Fructose Dehydration to HMF. *J. Energy Chem.* **2013**, *22*, 305−311.
(60) Zhang, J.; Liu, X.; Blume, R.; Zhang, A.; Schlogl, R.; Su, D. S. Surface-Modified Carbon Nanotubes Catalyze Oxidative Dehydrogenation of N-Butane. *Science* **2008**, *322*, 73−77.
(61) Hulicova-Jurcakova, D.; Puziy, A. M.; Poddubnaya, O. I.; Suarez-Garcia, F.; Tascon, J. M.; Lu, G. Q. Highly Stable Performance of Supercapacitors from Phosphorus-Enriched Carbons. *J. Am. Chem. Soc.* **2009**, *131*, 5026−5027.
(62) Patel, M.; Savaram, K.; Keating, K.; He, H. Rapid Transformation of Biomass Compounds to Metal Free Catalysts *via* Short Microwave Irradiation. *Journal of Natural Products Research Updates* **2015**, *1*, 18−28.

DOI: 10.1021/acsnano.5b07054
ACS Nano 2016, 10, 2305−2315